19930093292

ACR Dec. 1940

NATIONAL ADVISORY COMMITTEE FOR AERONAUTICS

WARTIME REPORT

ORIGINALLY ISSUED

DRAG AND PROPULSIVE CHARACTERISTICS OF AIR-COOLED ENGINE-NACELLE INSTALLATIONS FOR TWO-ENGINE AIRPLANES

By Herbert A. Wilson, Jr., and Robert R. Lehr

Langley Memorial Aeronautical Laboratory
Langley Field, Va.

NACA

WASHINGTON

NACA WARTIME REPORTS are reprints of papers originally issued to provide rapid distribution of advance research results to an authorized group requiring them for the war effort They were previously held under a security status but are now unclassified. Some of these reports were not technically edited. All have been reproduced without change in order to expedite general distribution.

DRAG AND PROPULSIVE CHARACTERISTICS OF RIB-COOLED ENGINE-NACELLE INSTALLATIONS FOR TWO-ENGINE AIRPLANES

By Herbert A, Wilson, Jr,, and Robert R. Lehr

SUMMARY

Research on wing-nacelle propeller arrangements has 'Seen continued in the NACA Cull-scale mind tunnel with tests on a model of a two-engine airplane provided with nacelles varying in diameter from 1.5 La 2.6 times the local wing thickness. This model is the same one that was previously tested with four-engine-nacelle installations, and the results are directly comparable.

The results show the variation of the nacelle drag with tho ratio of t'ne nacelle diameter to the wing thickness, the effects of the nacelles on the aerodynamic characteristics of the airplane, and the propulsive and tie over-all efficiencies for all the arrangements. The present results are combined. in some cases with the results of previous experiments, so that the effect of nacellesis included for airplanes ranging from 6½ to 100 tons.

INTRODUCTION

The tendency to increase the power or" radial air-cooled airplane engines without increasing the engine diameter has led to large variations in the size ol the wing nacelles relative to the size of the wing. An investigation conducted in the WACA full-scale wind tunnel has dealt with the Influence of the ratio of the nacelle diameter to the wing thickness and of the longitudinal and vertical propeller location on the drag, the propulsive efficiency, and the over-all efficiency of multiengine airplanes. The effects of the nacelles and the propeller operation on the lift and the pitching moment of the airplane have also been studied. The investigation covered ratios of the nacelle diameter to the wing thickness varying from 0.53 to 2.60, representing airplanes of from 6½ to 100 tons gross weight.

By variation of t'ne number and size of the nacelles installed on the same airplane model, a series of airplanes has been represented from which directly comparable data were obtained. The tests of these models were divided into

two groups: The first group, reported in reference 1, consisted of tests of the model with four nacelles of diameters varying from 0.53 to 1.5 times the wing thickness; the second group, constituting the basis for this report, covers tests of the model with two nacelles of diameters varying from 1.5 to 2.6 times the wing thickness.

SYMBOLS

α angle of attack of the fuselage reference axis relative to the wind axis, degrees

q free-stream dynamic pressure, pounds per square foot

S wing area, square feet

$\bar{c}$ mean chord of wing, area/span, feet

t_w maximum wing thickness (average over nacelle), feet

D_P propeller diameter, feet

D_N maximum nacelle diameter, feet;

F maximum cross-sectional area of nacelle, square feet

V air speed, feet per second

L lift, or force normal to the relative wind, pounds

D drag, or force parallel to the relative wind, pounds

D_c power-off drag of model with engine-nacelle installation, pounds

M pitching moment, pound-feet

$$C_L = \frac{L}{qS}$$

$$C_D = \frac{D}{qS}$$

$\Delta C_D = C_{D_c} - C_{D_w}$ (Subscript w refers to power-off drag of the model with bare wing; subscript c, to power-off drag of model with engine-nacelle installation)

$C_{D_F} = \frac{\Delta C_D S}{2F}$

$C_m = \frac{M}{qS\bar{c}}$

R resultant force of a propeller-nacelle-wing combination, pounds

T thrust of propellers operating in front of a body (tension in propeller shafts), pounds

A3 increase in drag of the body due to the action of the propellers, pounds

T-ΔD effective thrust of the propeller-nacelle installation

P power input to all propellers

$\eta = \frac{(T - \Delta D)V}{P}$ propulsive efficiency

$\eta_t = \eta \left(\frac{C_{D_w}}{C_{D_c}}\right)$ over-all efficiency

$T'_{c_o} = \frac{P\eta_o}{\frac{\rho}{2} V^3 S}$ Index thrust coefficient

$\eta_o = \eta$ at $C_L = 0.25$

n propeller speed, revolutions per second

β propeller-blade angle at 0.75 radius, degrees

δ_f flap deflection from closed position, degrees

MODEL AND TEST EQUIPMENT

The tests were conducted in the NACA full-scale wind tunnel, which is described in reference 2. The model is a notal-covered, midwing monoplane with a span of 87.25 feet, The symmetrical wing sections are tapered in thickness from the NAGA 0018 at the root to the NACA 0010 at the tip. The wing plan form tapers 4:1 from a root chord of 7.28 feet, aod the wing area, is 172 square feet. Split trailing-edge flaps extend over the middle 60 percent of the span mith the exception of a short gap at the fuselage. The angle of the wing setting to the fuselage reference line is 4.6°. The principal dimensions of the model and the nacelle for each of the test arrangements are shown in figure 1. Figures 2 to 6 show the model as installed in the full-scale tunnel.

A summary of the nacelle arrangements tested *is* shown in table I.

TABLE I

Test	Nacelle diameter (in.)	$\frac{D_N}{t_w}$ (1)	Propeller diameter (in.)	$\frac{D_N}{D_P}$	Propeller location (2)	Nacelle position	Details in
1	No cowling -		Bare-wing model				fig. 2
2a	20	1.5	48	0.417	0.25c	Center line	fig. 3
2b	20	1.5	48	.417	.25c	Low	fig. 4
3	30.4	2.27	69	.440	.50c	Center line	fig. 5
4	34.7	2.6	84	.413	.50c	Center line	fig. 6

[1] Thickness t_w is the average of wing thickness at the nacelle locations,

[2] Chord c is the local chord at each propeller location.

Power to operate the propellers was furnished for the 20-inch nacelle arrangement by the 25-horsepower alternating-current motors used in the tests of reference 1, and for the \$0.4-inch and 34.7-inch nacelle arrangements by 15-horsepower motors of lower synchronous speed. For all three nacelle arrangements, the motors were supported ahead of the wing and within the nacelles. The propeller speed mas regulated by varying the frequency or" the motor-current supply and was measured with an electric tachometer. Power output was obtained for the 25-horsegoner motors from an electrical calibration and for the 15-horseyotver motors by measurement of the torque reaction on the motor.

Three sets of propellers, a modified Bureau of Aeronautics Drawing No. 4412 two-blade propeller of 48-inch diameter, a Curtiss 88980 three-blade propeller of 69-inch diameter, and a Hamilton Standard 1827 two-blade propeller cut down from an 8- to a 7-foot diameter, were used on the 20-, the 30.4-, and 34.7-inch nacelles, respectively.

The contour of the cowlings and their relative dimensions are given in figure 7 as fractions of the cowling diameter, These cowlings were geometrically similar to those used in the previous series of tests (reference 1) and to the one designated cowling C in reference 3. The shapes of the nacelles were designed in each case to avoid flow separation on the afterbody. At the intersection of the nacelle and the wing plasticine fillets of small radius mere used to provide a smooth fairing.

Perforated metal plates, the resistance of which was changed to a value of conductance K (reference 4) of approximately 0.10, simulated the engine. The exit slot of the cowling was proportioned to give a pressure drop of 0.030q across the engine; it was assumed that a means of exit-slot adjustment such as flaps would be provided for other flight conditions. For the tests with no cooling air, the exit slot was sealed to prevent any air flow through tho cowling. This method was found to give more consistent results than sealing the perforation in the metal plates of the engine, as was done for the tests of reference 1; the improvement can be attributed to a better flow condition at the exit slot.

TESTS

With propellers removed from %he model, measurements of aerodynamic characteristics mere made at an air speed of about 60 miles per hour for each of the nacelle installations over an angle-of-attack range from zero lift through the stall, Scale effect on the drag at low lift coefficients was also measured over a range of air speeds from 30 to 100 miles per hour.

With the propellers operating, propulsive characteristics of the nacelle-propeller installations were determined for the attitude in which the thrust axes were parallel to the relative wind and for lift coefficients approximating those for the high-speed and the climbing conditions, The power-on measurements included the power input to the propellers and the propeller speed as well as the usual aerodynamic forces and moments. For the propulsive efficiency tests, the V/nD was varied by increasing the air speed from 30 to 100 miles per hour and then by decreasing the propeller speed at the masimum air speed until zero torque was obtained. The effect of propeller operation on the lift and on the pitching moment was determined nt a test air speed of approximately 60 miles per hour for the maximum thrust permitted by the set-up and for an intermediate thrust condition,

POWER-OFF CHARACTERISTICS

The aerodynamic characteristics of the two-engine model with the propellers removed are shown in figures 8 to 12 for tho various arrangements tested. These data were obtained at a tunnel air speed of about 60 miles per hour, which corresponds to a Reynolds number of about 2,500,000 based on the average wing chord of 4.62 feet. The coefficients are based on a wing area of 172 square feet and are corrected for wind-tunnel effects. Pitching-moment coefficients are computed about a center of gravity located as shown in figure 1.

Drag.- Scale effects on the airplane drag coefficients for the nacelle arrangements and for the model without nacelles, tested at an assumed high-speed lift coefficient of 0.25 are given in figure 13. A comparison of the curves for the various nacelle installations with those for the

bare wing shows that the drag increment due to the nacelles is more or less independent of the test air speed within the range covered.

The variation of the nacelle drag increment per nacelle $\Delta C_D/2$ with the ratio of the nacelle-diameter to the wing thickness D_N/t_w is shown in figures 14(a), (b), (c), and (d) for the present tests at lift coefficients of -0.04, 0.25, 0.5, and 0.7, together with similar data from the earlier tests of reference 1. The propeller location for nacelle arrangements with values of D_N/t_w of 2.27 and 2.60 was 0.50c ahead of the leading edge of the wing as compared with a position of 0.40c for the other nacelles of figures 14(c) and (d). The difference in drag between the nacelles with the propeller positions of 0.40c and of 0.50c has been disregarded in the discussion of the variation of the nacelle drag coefficient and will *be* examined later. The increase in the total drag due to nacelles of large relative diameter as well as the importance of the drag due to *tho* flow of the cooling air for large values of D_N/t_w is clearly shown in figure 14.

The nacelle drags are also shown in terms of the nacelle drag coefficient C_{D_F} in figure 15, from which figure the drag of conventional nacelle and cowling installations can be predicted. There is a large increase in nacelle drag coefficient with lift coefficient for small values of D_N/t_w. As the value of D_N/t_w increases, %he nacelle drag coefficient tends to approach a constant value and to become considerably less dependent on the Lift coefficient and the propeller position.

The nacelle drags without cooling air flowing were considerably smaller for the two-nacelle tests than for the four-nacelle tests of reference 1. This difference is particularly noticeable for the 20-inch nacelles with the 0.25c propeller position because a direct comparison is shown, The decrease in nacelle drags is attributed to sealing the cowling exit for the present tests rather than sealing the perforated metal plates, thus eliminating secondary flows due to pressure differences around the periphery of the cowling exit,

Calculations of the drag due to forcing air through the cowling and the perforated plate simulating the engine, as outlined in reference 4, give increases in the

nacelle drag coefficient of 0.020 and 0.014 for the 34.7- and the 30.4-inch nacelles, respectively, that check remarkably well nith the values of 0.019 and 0.014 from the data of figure 15.

An unexpected decrease in drag mas shown by the 20-inch nacelles in the loa position (fig. 13). This decrease is inconsistent with the results of recent tests made in the NACA 8-foot Sigh-speed tunnel (reference 5) that show a 2-perceat increase in the airplane drag for lowering the nacelle. For t'ne tests of reference 5, the lowered nacelle was qeometrically similar to the center-line nacelle; whereas, in the present tests the nacelle afterbody mas faired to provide additional space in the nacelle for housing the landing gear. This requirement of space made it necessary to elongate the nacelle and to fair from the circular engine section to a vertical line at the tail. It is believed that the more gradual fairing of the low nacelle caused- less interference between the mine and the nacelle on the lower surface and that lowering the nacelle decreased the interference on the upper surface of the wing to a low value. This conclusion is partially verified by the fact that the drag for the lowered nacelle approaches more nearly the skin-friction drag for a corresponding amount of surface in turbulent flow.

Maximum lift.- The maximum lift coefficient was slightly decreased (about 1 percent) by the addition of the nacelles to the airplane. Table II summarizes the maximum lifts for all the test arrangements.

TABLE II

Values of Maximum Lift Coefficient

D_N/t_w	Propeller location	Flap deflection, δ_f		
		0°	60°	Vertical position
Bare wing		1.29	1.82	
1.50	0.25c	1.28	1.77	Center line
1.50	.25c	1.28	1.76	Low
2.27	.50c	1.27	--	Center line
2.60	.50c	1.26	--	Center line

L-428

A comparison of the values for the current tests with those for the tests of reference 1 shows a considerable difference in the effect of the nacelles on maximum lift, Adding four 20-inch nacelles to the model gave a decrease in maximum lift of 9 percent; this decrease is inconsistent with the results of the two-nacelle tests. Tuft surveys (fig. 16) chow that the nacelle has a marked effect on the direction of flow over the toy of the wing, and it is reasonable to conclude that two nacelles only a short distcnce apart have a mutual intarference flow that, at high angles of attack, causes an early separation on the upper surface of the wing. It is also evident from the two-engine tests that the interference is not serious for an isolated wing nacelle.

Lift-drag ratio.- The range of an airplane is about proportional to the value of the maximum lift-drag ratio, which decreases rapidly with increasing D_N/t_w, as shown in figure 17. The maximum L/D for the 20-inch nacelle ($D_N/t_w = 1.5$) is 15 percent lower than that for the bare wing while the L/D 34.7-inch nacelle ($D_N/t_w = 2.6$) is 20 percent lover. The four-engine data of reference 1, also included- in figure 17, show the lift-drag ratio for the four 20-inch-nacelle installations to be approximately 25 percent less than for the bare wing.

Pitching moment.- The destabilizing effect of large nacelles is apparent in figure 18, in which the slopes of *the* pitching-moment coefficient curves are plotted against D_N/t_w. The slopes were read over the straight portions of the pitching-moment curves at values of α between -5° and 5°, the decreased stability being indicated by the lower values of negative slope. The curves include, in addition to the results of the present nacelle and bare-wing tests, similar data obtained with four nacelles in reference 1. The results were found to be much more critical for the four-nacelle conditions.

The decrease noted in *the* slope of the pitching-moment curve is attributed to the forward movement of the aerodynamic center of the wing due to the addition of the nacelles ahead of the leading edge. Consequently, moving the nacelles ahead from a propeller position of 0.25c to one of 0.40c or 0.50c further accentuates the destabilizing effect of the nacelles.

PROPULSIVE AND OVER-ALL EFFICIENCIES

The nacelle drag coefficients alone are an insufficient basis for comparison of the various nacelle-propeller installations. The installations are more properly compared by means of an over-all efficiency that includes tho nacelle drag increment measured with the propeller removed as well as the propulsive efficiency. This over-all efficiency η_t is defined as the ratio of the towline power required for the model without nacelles at a given level-flight speed to the actual power input required at this speed by the model with the nacelle-propeller installation. The over-all efficiency is therefore written

$$\eta_t = \eta \left(\frac{C_{D_w}}{C_{D_c}} \right)$$

The propulsive efficiency η is the ratio of the effective thrust power to the power input and may be calculated from the relation

$$\eta = \frac{(T - \Delta D)\ V}{P}$$

The value of t'ne effective thrust, $(T - \Delta D)$, can be computed from *the* mind-tunnel data by the relationship

$$T - AD = D_c + R$$

in which D_c and R are, respectively, the values of the drag for propeller-removed and propeller-operatin? conditions.

The drag increment included. in the effective thrust is caused by the slipstream over the wing; in like manner a lift increment is attributed to the propeller operation. In order to correct for this lift change, D_c and R mere both measured at *t'ne* same lift coefficient rather than at the same angle of attack.

Propulsive Efficiencies

Data have been obtained from the tests to show the effect on the propulsive efficiency of variations in the pro-

peller blade angle, the nacelle diameter, and the lift coefficient.

Propeller blade angle.- The values of the propulsive efficiencies measured for the various nacelle-propeller combinations are shown in figures 19 to 32. The maximum propulsive efficiencies occur at a blade angle β of about 30°; the envelopes of the propulsive-efficiency curves are reasonably flat, however, showing only slight variations in efficiencies with a variation in β of $\pm 10^\circ$ from the optimum.

The results show that neither the blade angle for maximum efficiency nor the quantitative value of maximum efficiency varies appreciably from that of the previous study of the four nacelle propeller installations.

Nacelle diameter.- A variation in the ratio of the nacelle diameter to the wing thickness has little effect on the maximum propulsive efficiency, Changing the vertical position also has a negligible effect on the maximum efficiency except to change slightly the V/nD at which maximum efficiency occurs. The efficiency at a lift coefficient of -0.04 for the 34.7-inch nacelles is approximately 2 percent lower than that for the 20-inch nacelles and about 1 percent lower than that; for the 30.4-inch nacelles.

Lift coefficients.- The variations in the propulsive efficiencies with airplane lift coefficient are also included in figures 19 to 22 for blade angles of 20°, 30°, and 40°. The maximum propulsive efficiency occurs at a lift coefficient of -0.04, in which case the nacelle axis was approximately parallel to the air stream. The propulsive efficiency in all cases except for the 20-inch nacelle with the blade angle set at 30° is 2 percent greater at the lift coefficient -0.04 than at 0.25. For the 20-inch nacelle with a blade angle of 30° the propulsive efficiency is the same for the two lift coefficients in either the center line or the lowered nacelle position.

Over-All Efficiencies

The over-all efficiencies for the conditions investigated during the present series of tests together with those of the previous series (reference 1) are presented in figure 23.

It will be noted that there is a 1- to 2-percent decrease in the over-all efficiency for the 0.40c propeller position. The decrease is probably due to the increased skin friction of the longer nacelle. It will also be observed that the over-all efficiency for the two-engine installation is considerably higher than that for the four-engine installation, especially at larger values of D_N/t_w. This difference in over-all efficiency is the result of the lower drag obtained mit?? two nacelles and indicates the desirability of using the smallest possible number of power units for a given total power output.

Variations of the maximum over-all efficiency with lift coefficient for the two-engine data of the present tests and for the four-engine data of the previous series (reference 1) are plotted in figure 24. In all cases shown, the lowest efficiencies exist at the high-speed condition; the efficiencies increase as the lift coefficient either increases or decreases from the hfqh-speed. condition. This increase in efficiency is more rapid with the 30.4- and the 34.7-inch nacelles, because of a smaller variation in drag with angle of attack for the larger nacelles.

POWER-ON CHARACTERISTICS

The effect of propeller operation on *the* aerodynamic characteristics of an airplane is primarily dependent on the amount of thrust delivered by the propellers and, for a given thrust, is relatively independent of moderate changes in blade angle, V/nD, propulsive efficiency, and propeller diameter. In order to describe the conditions of propeller operation, use is made of an index thrust coefficient that takes the farm

$$T'_{C_O} = \frac{P\eta_O}{qSV}$$

in which η_O is the propulsive efficiency at $C_L = 0.25$ for the conditions of V/nD and blade angle at which the tests mere made. The index thrust coefficient has the characteristics and the form of a drag coefficient and is essentially independent of the combination of V/nD and blade angle that produces the thrust; it is equal to the amount of drag that the thrust would counterbalance at the

standard or index condition and, at any other value of lift coefficient, differs from the true thrust coefficient only by the variation in propulsive efficiencg between tho two conditions.

L-423

The effect of propeller operation on the maxinum lift is given in figures 25 and 26 for the 20-inch and the 30.4-inch nacelle installations. As t'e index thrust coefficient increases, the slope of th. lift curve increases slightly and the maximum lift increases rapidly. The rate of increase in maximum Lift coefficient is largest for values of T'_{c_o} between 0 and 0.05, owing to the effect of the slipstream in decreasing the wing-nacelle interference,

The effects of the propeller operation on the pitching-moment coefficient, for the various thrust coefficients and two nacelle installations, are shown in figures 27 and 28. The principal effect of propeller operation is to change the elevator angle required for balance. Tho curves are similar throughout the normal range of angles of attack and. are very much like those that would bo obtained by varying the tail setting, Increasing the nacelle size from 20 inches to 30.4 inches decreases the slope of all of the power-on pitching-moment curves. With the largest value of T'_{c_o} for each case, and especially with the larger nacelle, the stability becomes critical at tho higher angles of attack.

PRESSURE 3ISTRIBUTION

The pressure distribution an the under side of the 20-inch and the 34.7-inch nacelles is given in figures 29 and 30, respectively. These data may be used as a guide in designing trapdoors on the bottom of conventional nacelles. Similar data for fuselag s are given for a large range of Mach numbers in reference 6,

Pressures are given in terms of the pressure coefficient, $P = \frac{p - p_o}{q}$ (in which p is the local pressure and p_o is the free-stream static pressure), plotted normal to the surfaco of the nacelle. The results are plotted to give the distribution over four cross-sectional planes of the nacelles, located as shown in figures 29(b) and 30(b), between the leading edge of the wing and the

trailing edge of the nacelles, The pressure distribution over *tho* longitudinal sections is **also *shown*** in **figures** 29(a) and 30(a) for the center-line sections to give an indication of the fore-and-aft pressure variations.

CONCLUSTONS

1. The over-all efficiency of the two-engine model decreased **linearly** with an increase in the ratio of the nacelle diameter **to** the wing thickness.

2, The propulsive efficiencies were substantially the same for all nacelle arrangements.

3. The static longitudinal stability was adversely affected by the addition of the nacelles to the wing and the operation of the propellers.

4. The addition of the two **nacelles** to the wing decrossed the maximum lift by **only** about 1 percent.

Langley Memorial Aeronautical Laboratory,
National Advisory Committee for Aeronautics,
Langley Field, Va.

REFERENCES

1. Silverstein, Abe, and Wilson, Herbert A., Jr.: Drag and Propulsive Characteristics of Air-Cooled Engine-Nacelle Installations for Large Airplanes. NACA Rep. No. 746, 1942.

2. DeFrance, Smith J.: The N.A.C.A. Full-Scale Wind Tunnel. Rep. No, 459, NACA, 1933.

3. Robinson, Russell G., and Becker, John V.: High-Speed Tests of Radial-Engine Cowlings. NACA Rep. No. 745, 1942.

4. Theodorsen, Theodore, Brevoort, M. J., and Stickle, George W.: Full-Scale Tests of N.A.C.A. Cowlings. NACA Rep. No. 592, 1937.

5. Becker, John V., and Leonard, Lloyd H.: High-Speed Tests of a Model Twin-Engine Low-Wing Transport Airplane. NACA Rep. No, 750, 1942,

6. Delano, James B.: Pressure Distribution on tho Fuselage of a Midwing Airplane Model at High Speeds. NACA TB No. 890, 1943.

L-428

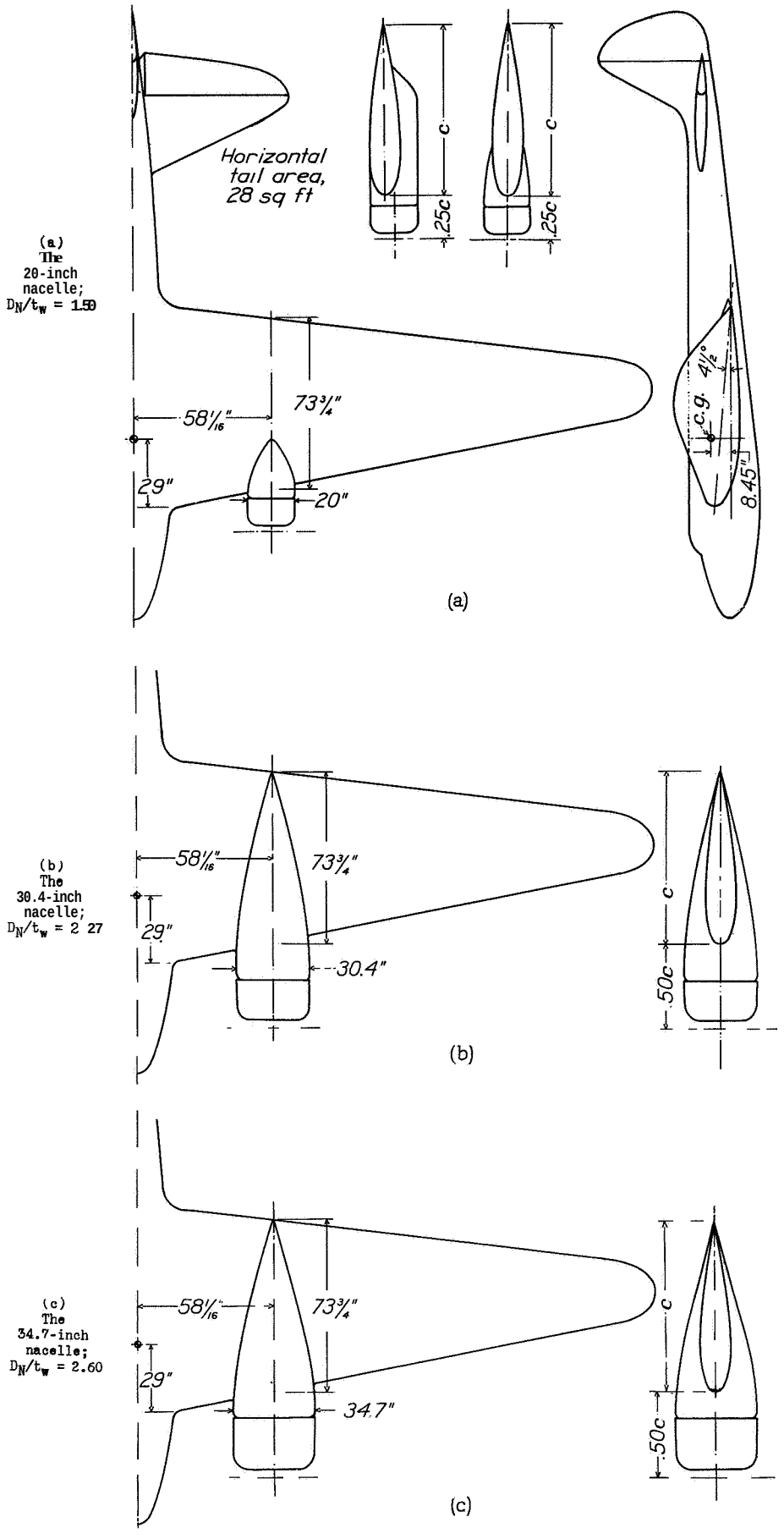

(a) The 20-inch nacelle; D_N/t_w = 1.59

(b) The 30.4-inch nacelle; D_N/t_w = 2.27

(c) The 34.7-inch nacelle; D_N/t_w = 2.60

Figure 1.

Diagram of model showing arrangements of the nacelles.

L-4478

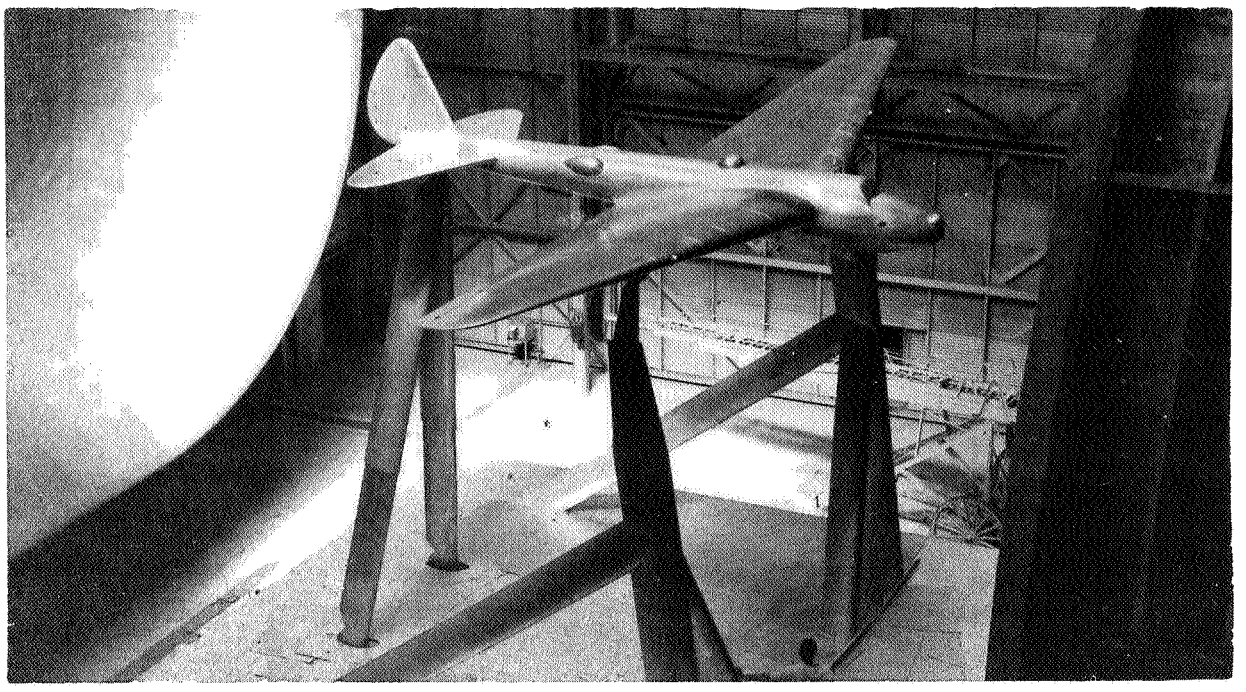

Figure 2.- Installation of model without nacelles in the NACA full-scale tunnel.

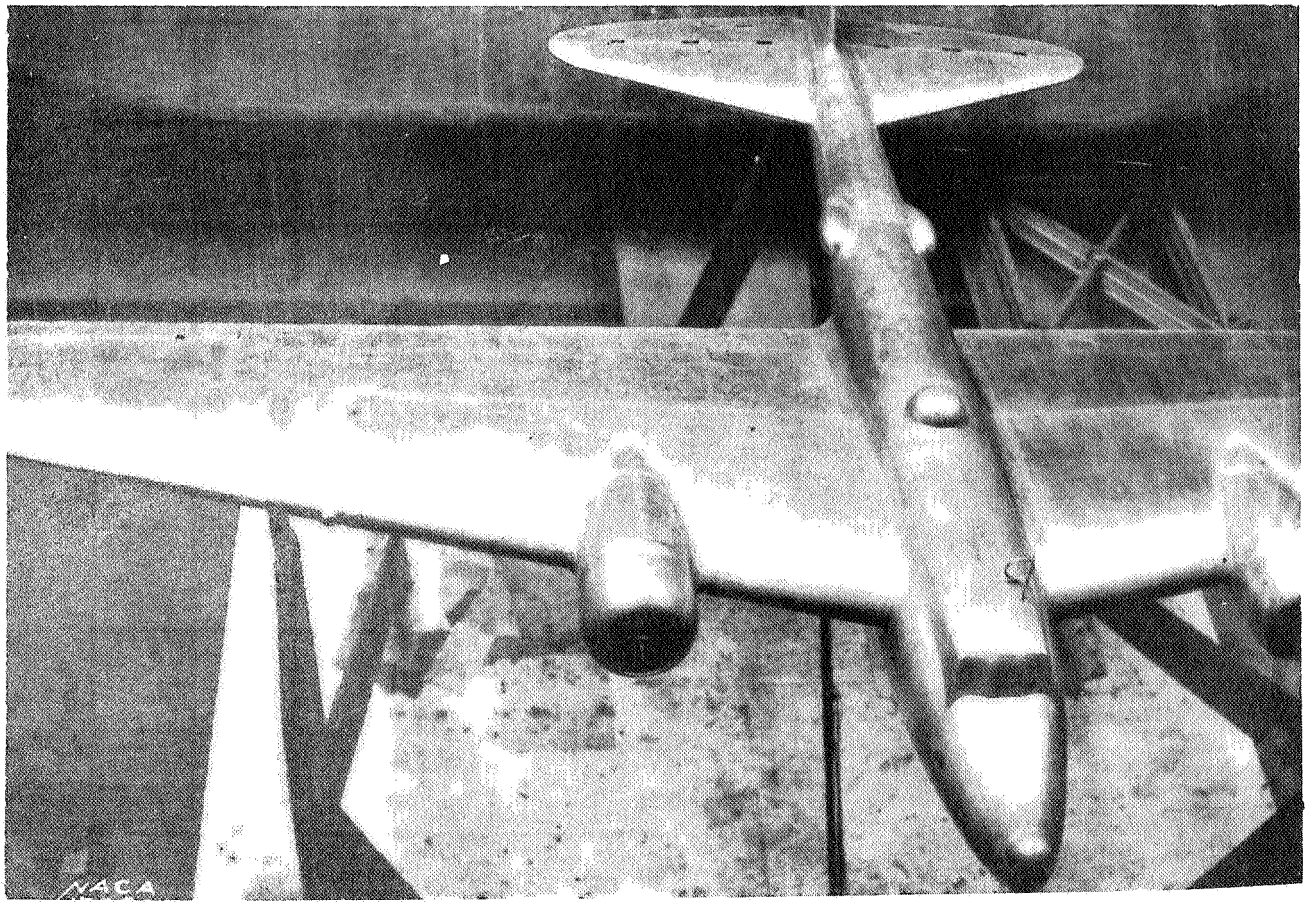

Figure 3.- Installation of model with 20-inch nacelles (center-line [illegible]) in the NACA full-scale wind tunnel.

L-428

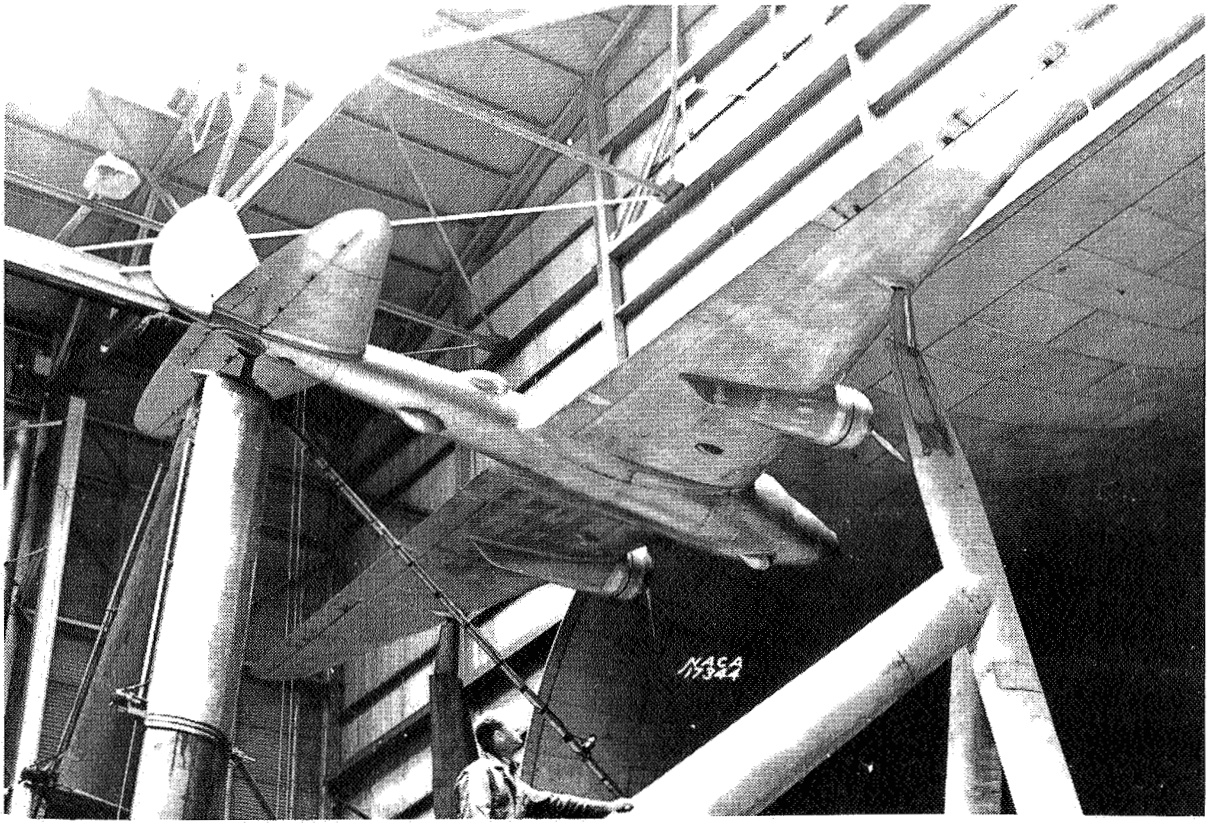

Figure 4.– Installation of model with 20-inch nacelles (low position) in the NACA full-scale wind tunnel.

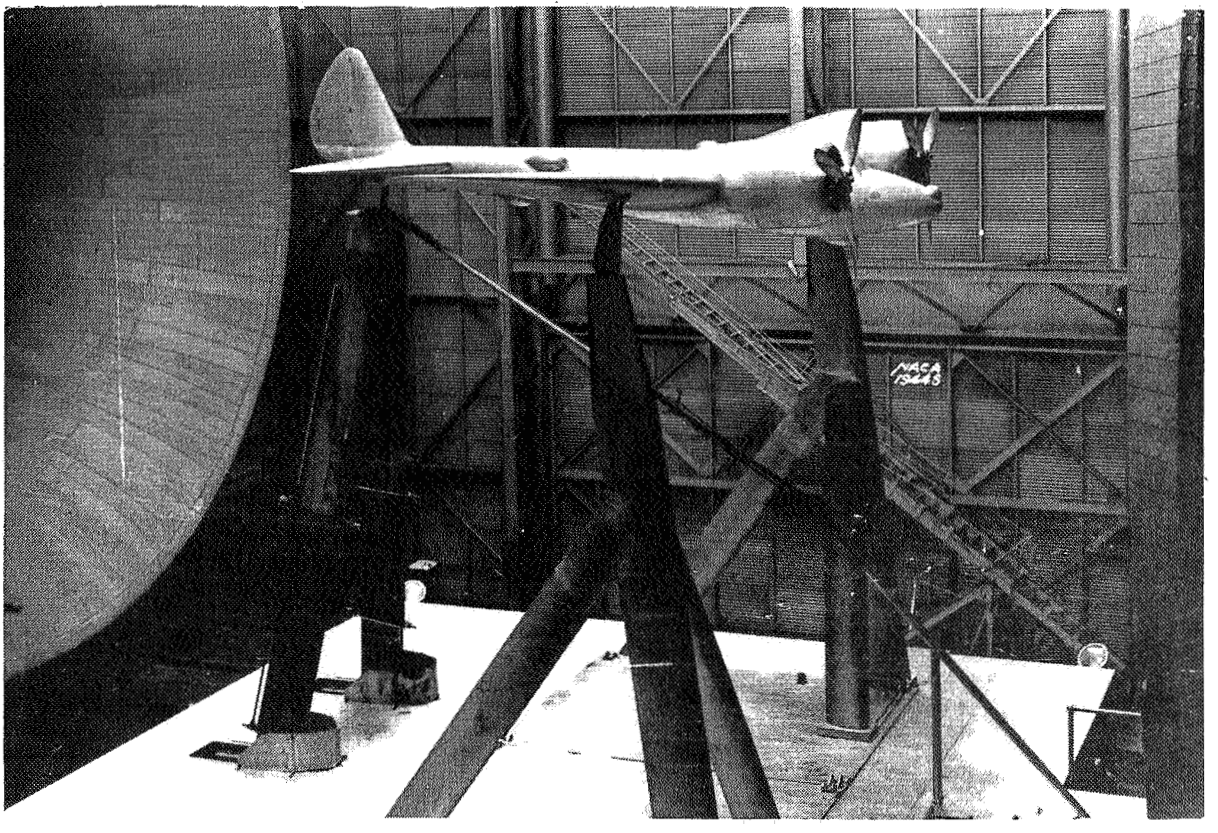

Figure 5. – Installation of model with 30.4-inch nacelles (center-line position) in the NACA full-scale wind tunnel.

4-428

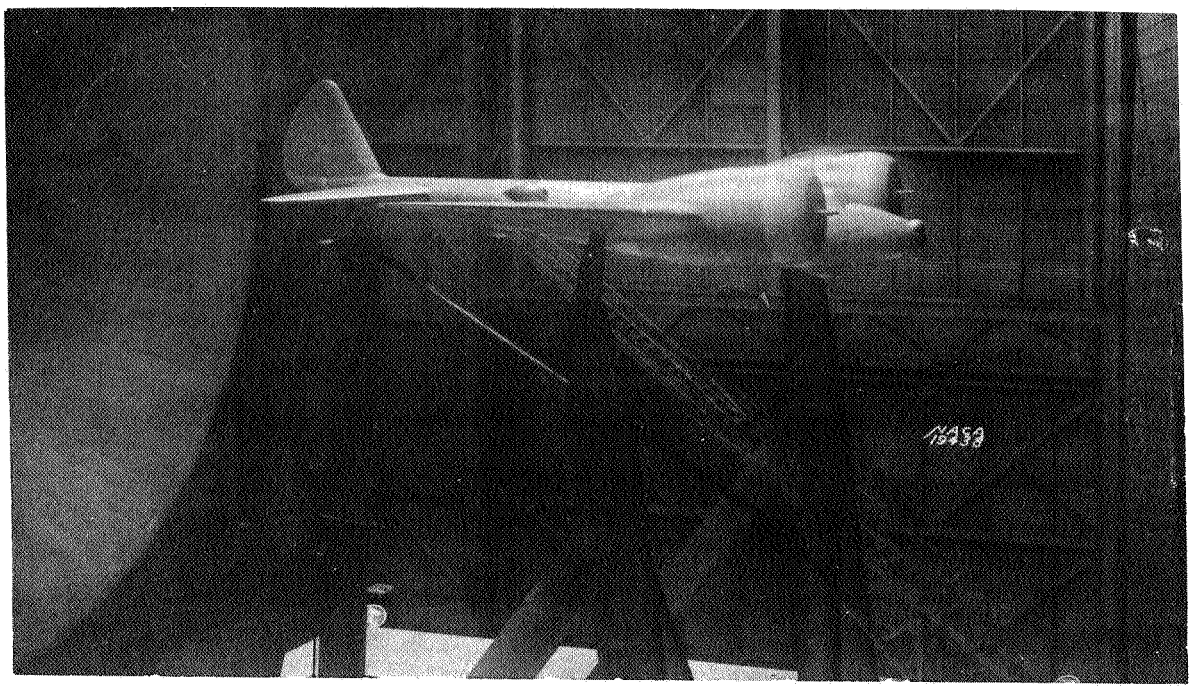

Figure 6.- Installation of model with 34.7-inch nacelles (center-line position) in the NACA full-scale wind tunnel.

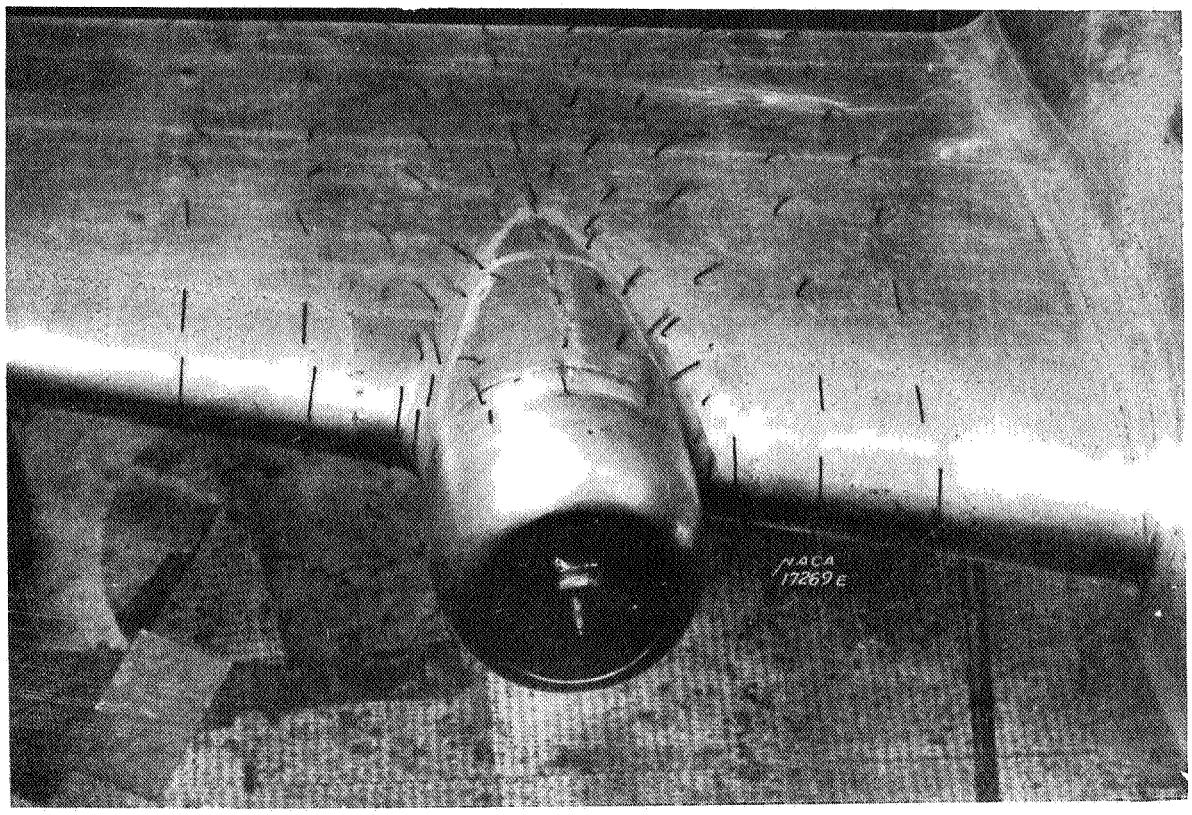

Figure 16.- Air flow over upper surface of wing and nacelle. The 20-inch nacelle: 0.25c propeller location; α = 3°

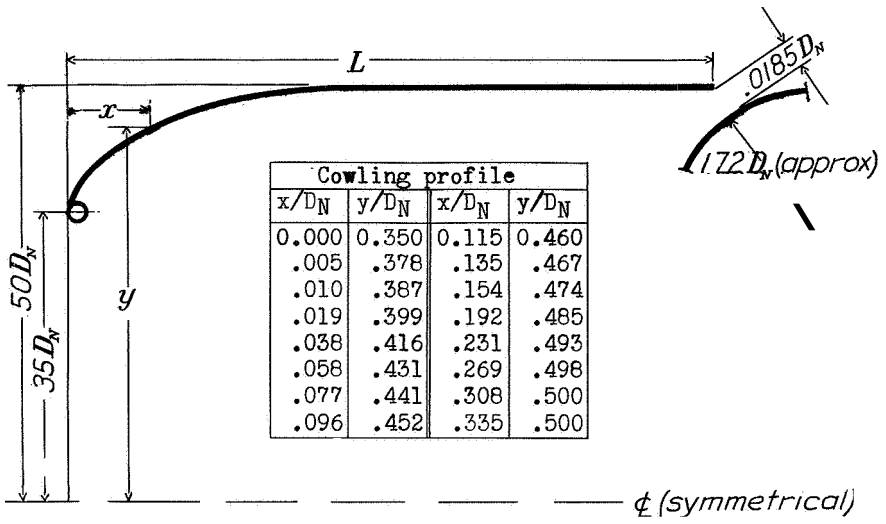

Cowling profile

x/D_N	y/D_N	x/D_N	y/D_N
0.000	0.350	0.115	0.460
.005	.378	.135	.467
.010	.387	.154	.474
.019	.399	.192	.485
.038	.416	.231	.493
.058	.431	.269	.498
.077	.441	.308	.500
.096	.452	.335	.500

Figure 7.- Dimensions of cowling and cooling arrangement.
L = 11.06 in. for 20.0 in. nacelle
" 16.69 " " 30.4- " "
" 22.00 " " 34.7- " "

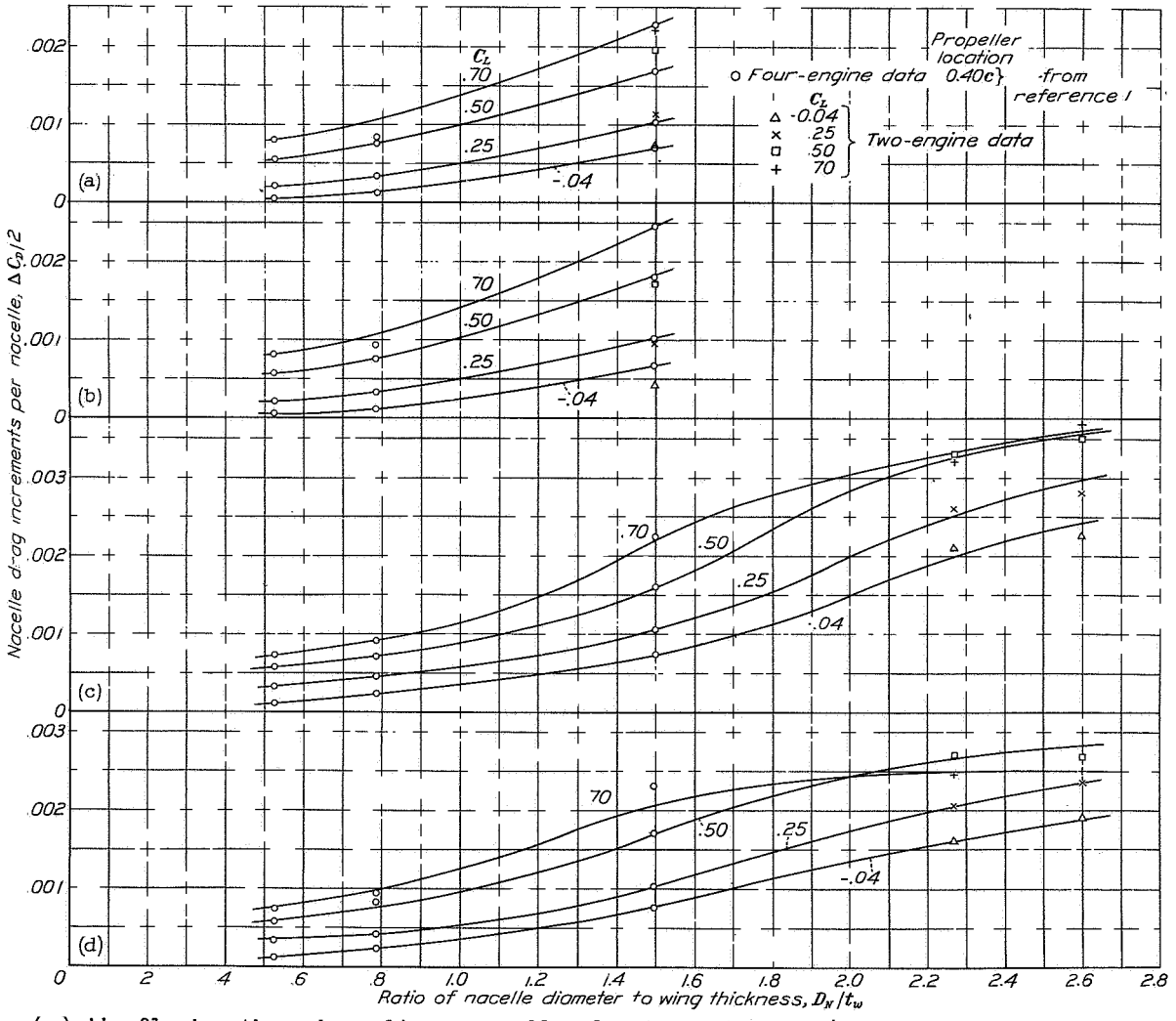

(a) Air flowing through cowling; propeller location, 0.25c. (b) Cowling closed; propeller location, 0.25c. (c) Air flowing through cowling; propeller location, 0.50c. (d) Cowling closed; propeller location, 0.50c.

Figure 14.- Drag increment due to each nacelle, $\Delta C_D/2$, for nacelles of various size and various lift coefficients. Test air speed, 100 mph.

L-428

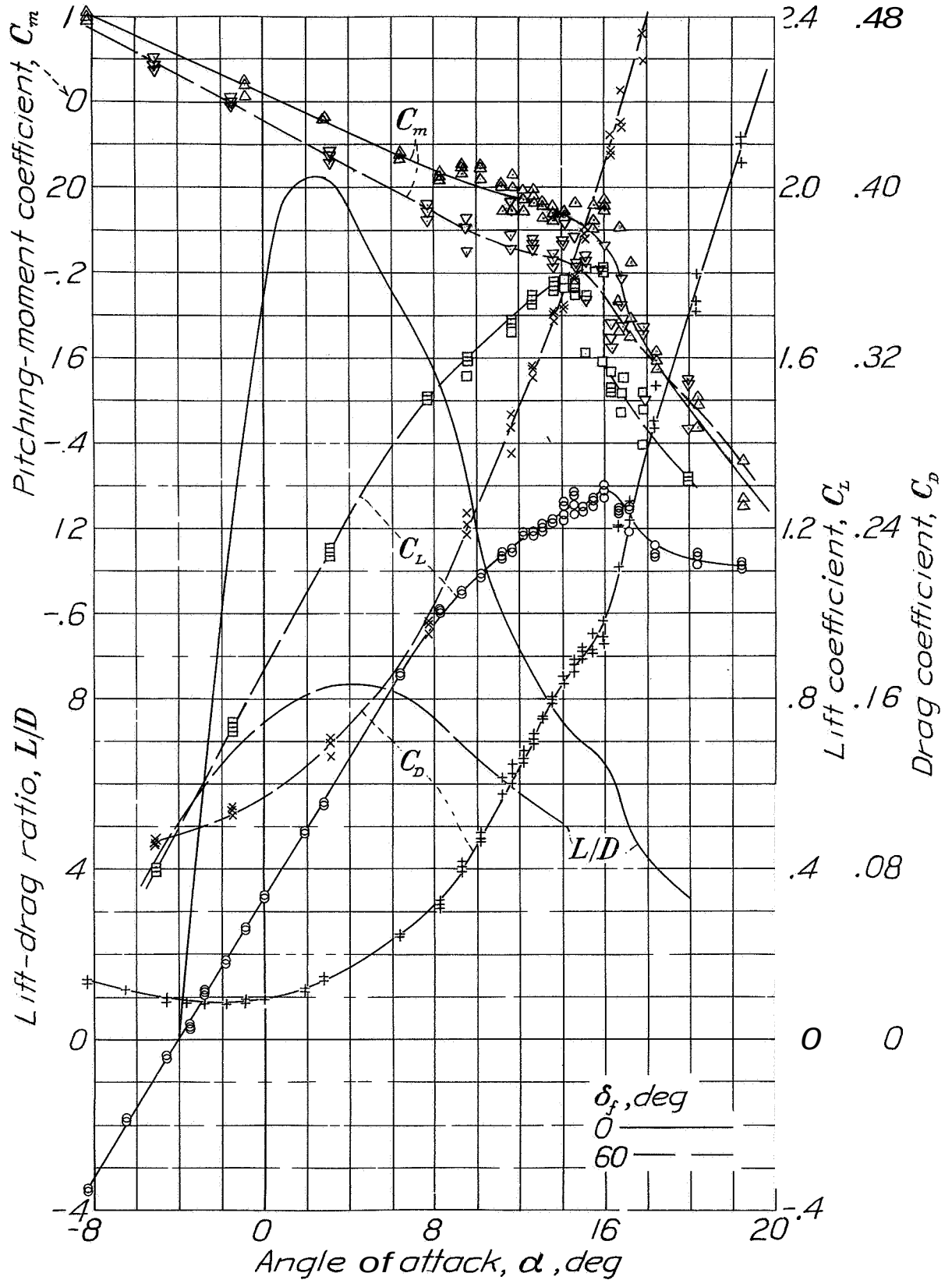

Figure 8.- Aerodynamic characteristics of model without nacelles. Approximate test air speed, 58 mph.

L-428

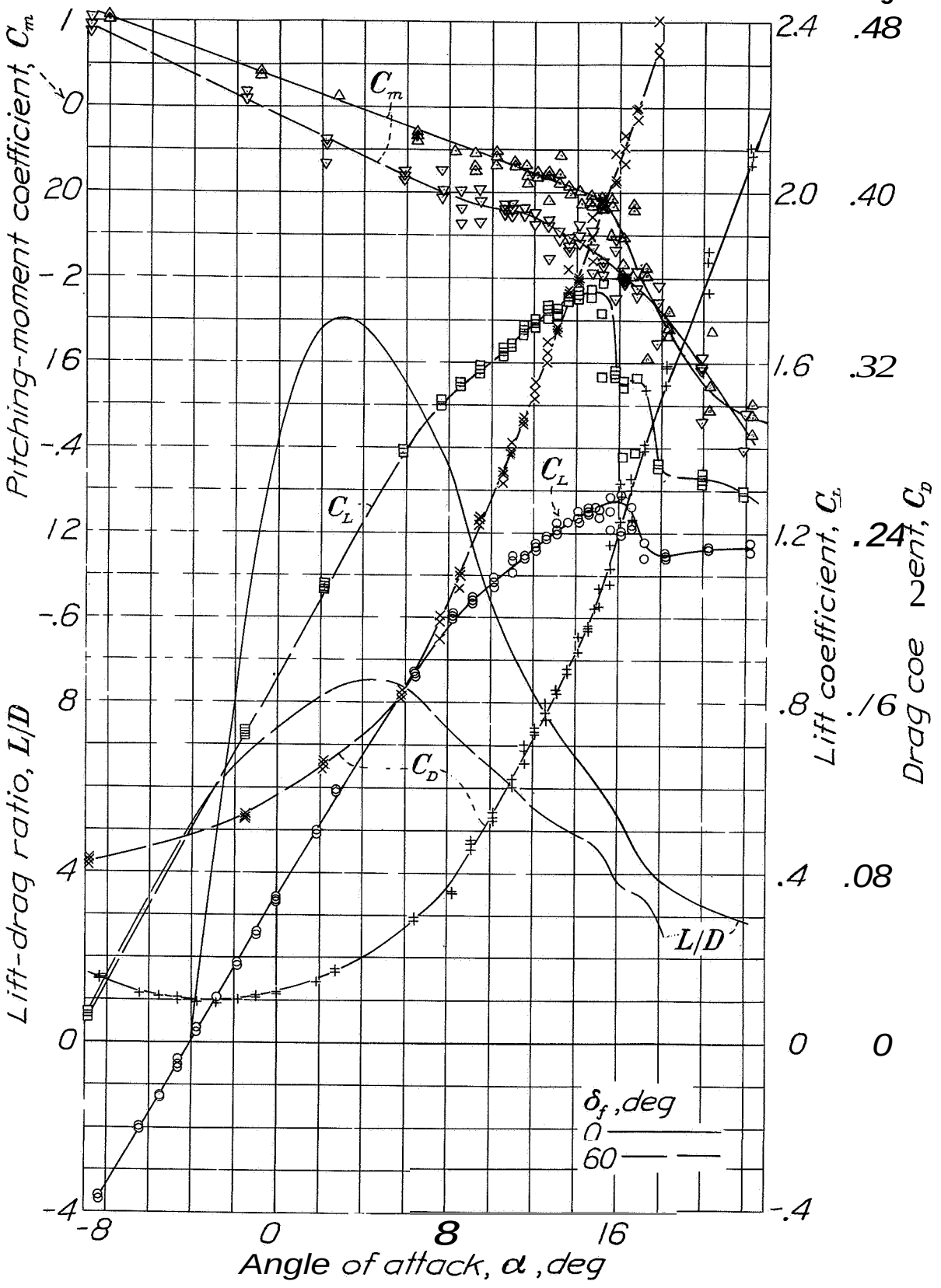

Figure 9.- Aerodynamic characteristics of model with 20-inch nacelles in center-line position. Approximate test air speed, 58 mph.

L-423

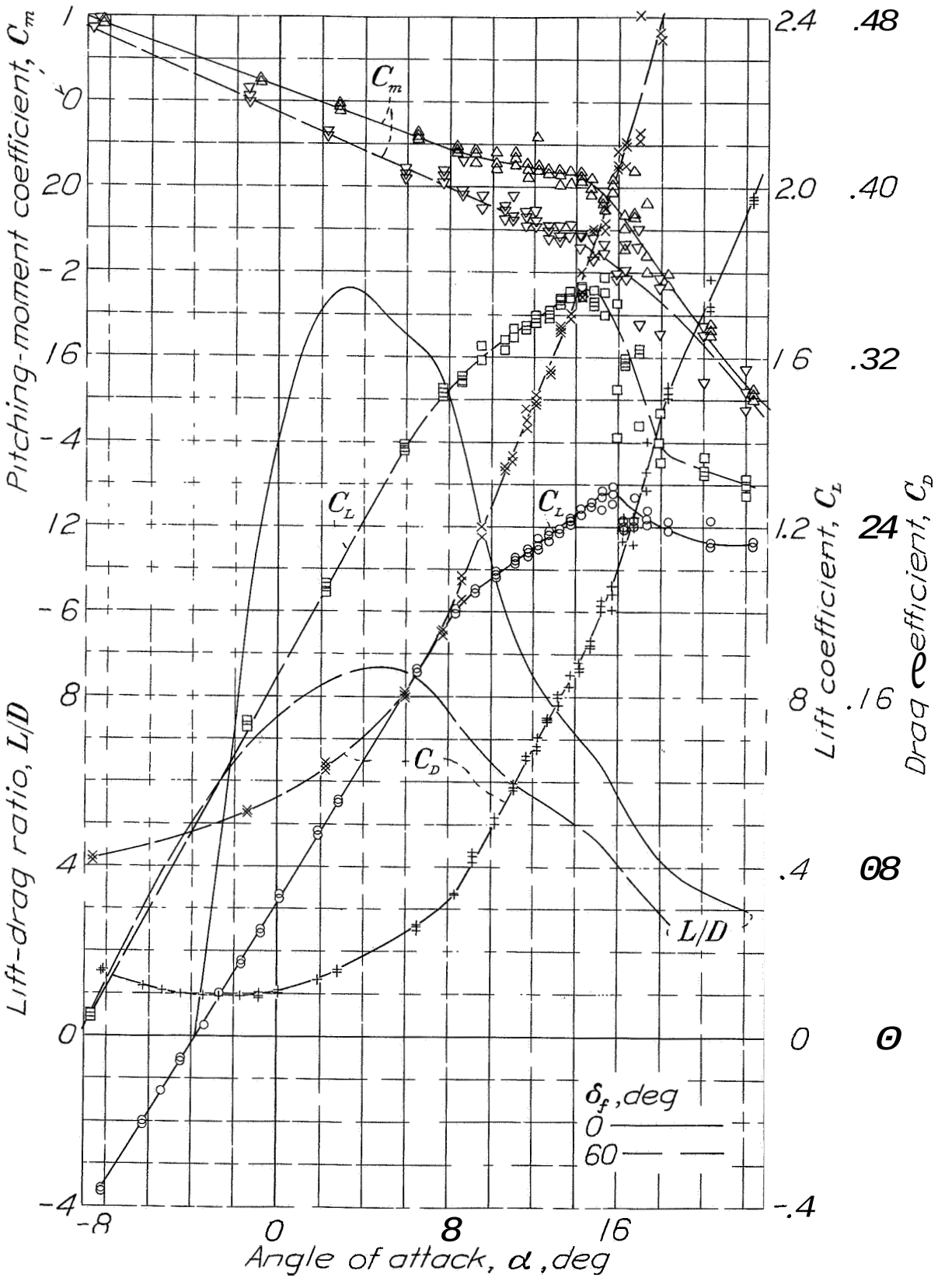

Figure 10.- Aerodynamic characteristics of model with 20-inch nacelles in low position. Approximate test air speed, 58 mph.

L-428

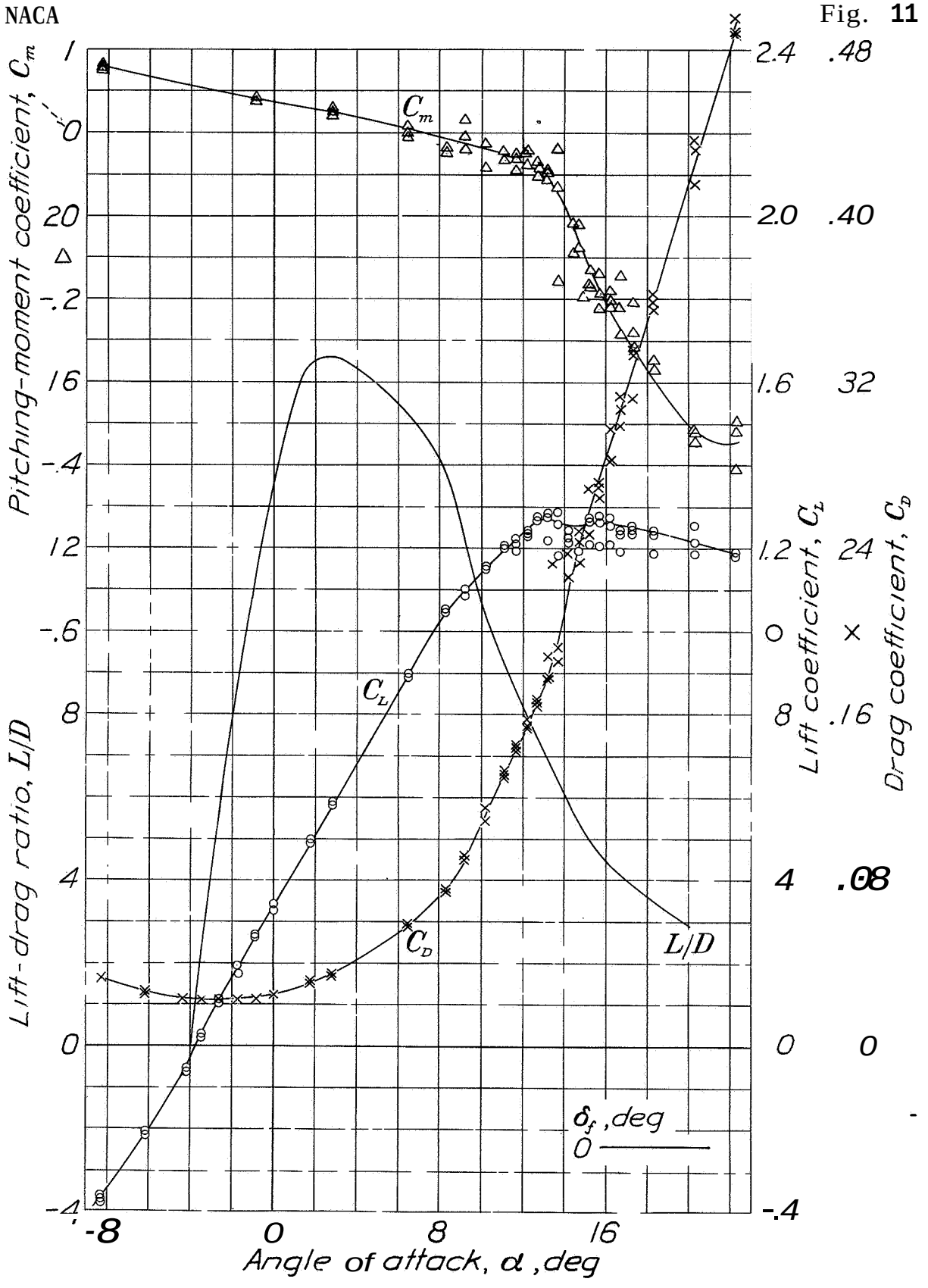

Figure 11.- Aerodynamic characteristics of model with 30.4 inch nacelles. Approximate test air speed, 58 mph.

L-428

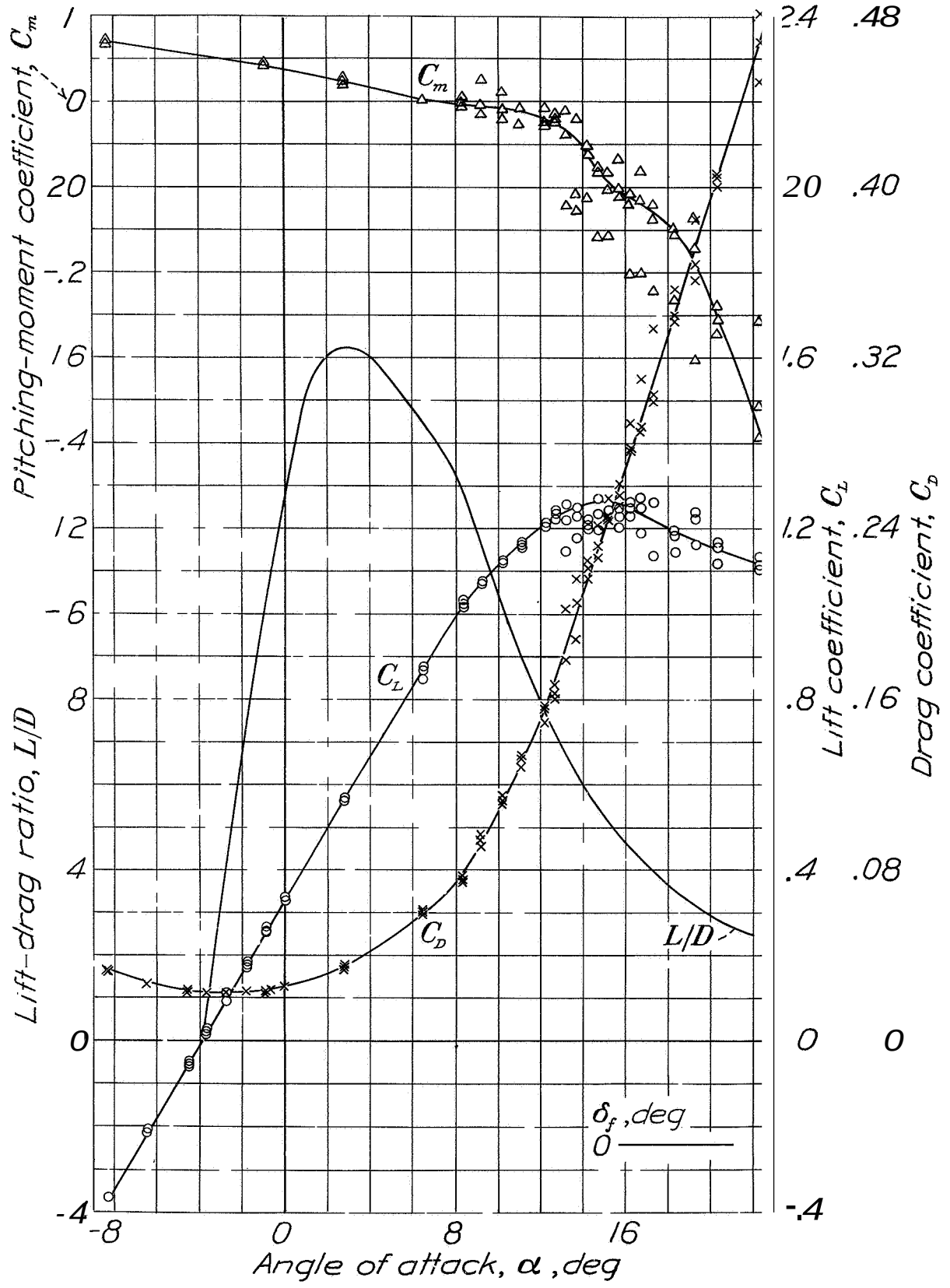

Figure 12.- Aerodynamic characteristics of model **with** 34.7 inch nacelles. Approximate test air speed, 58 mph.

L-4.28

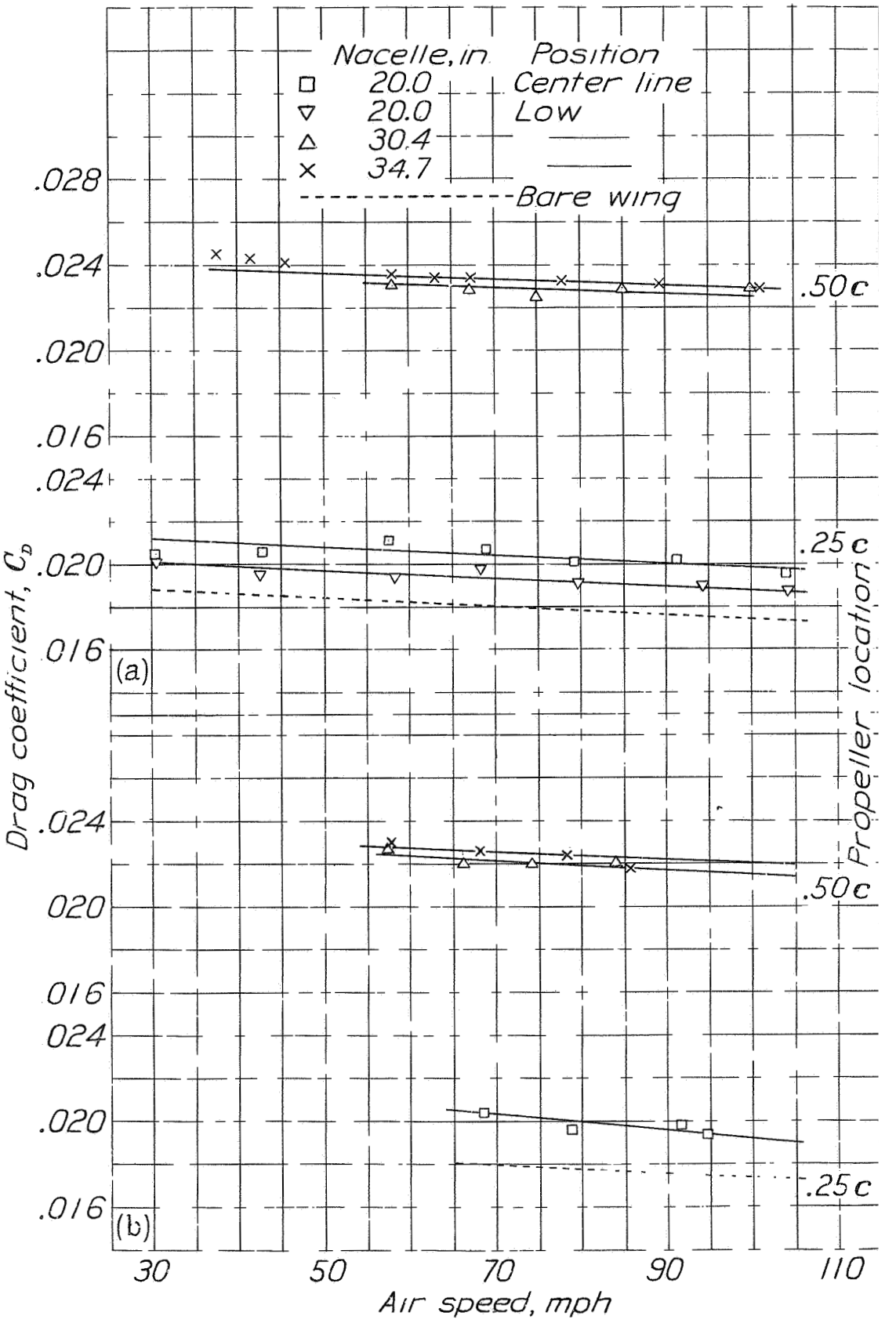

Figure 13.- Scale effect **on** drag **coefficient** at $C_L = 0.25$.

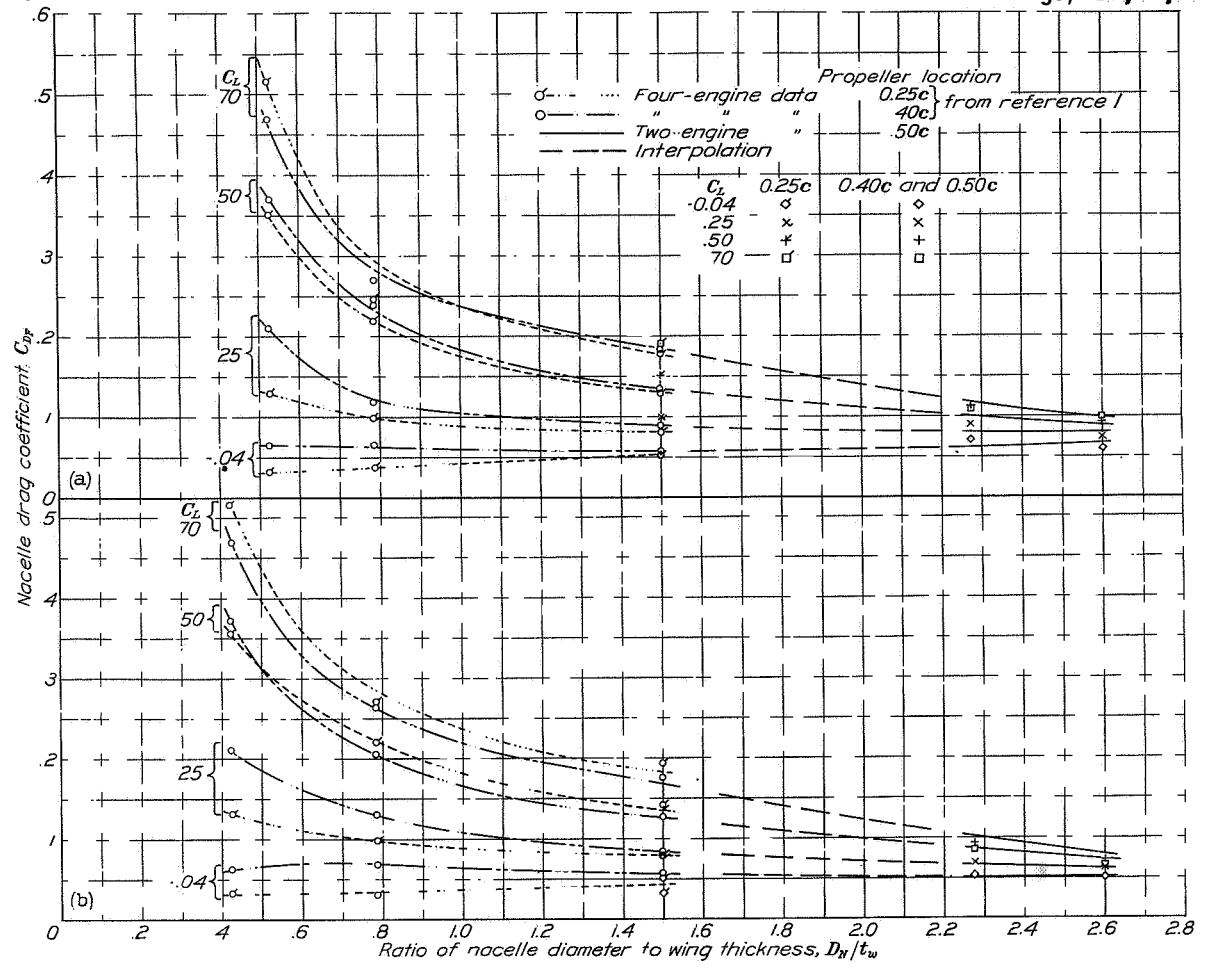

(a) Air flowing through cowling (b) Cowling closed

Figure 15.- Nacelle drag coefficient for various size nacelles and lift coefficients. Center-line nacelles.

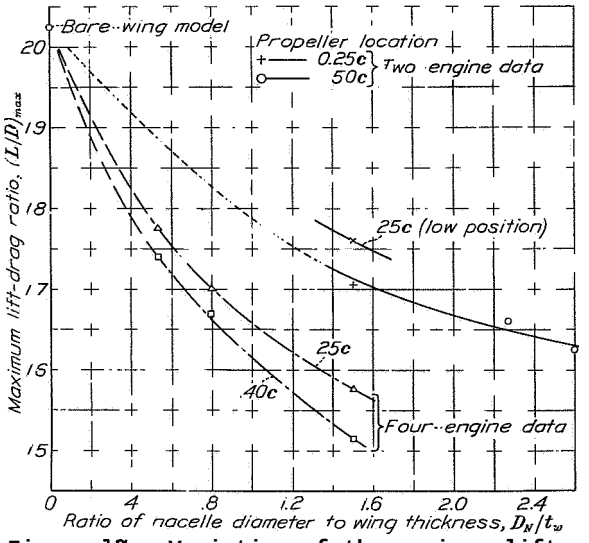

Figure 17.- Variation of the maximum lift-drag ratio of the model for various nacelle sizes.

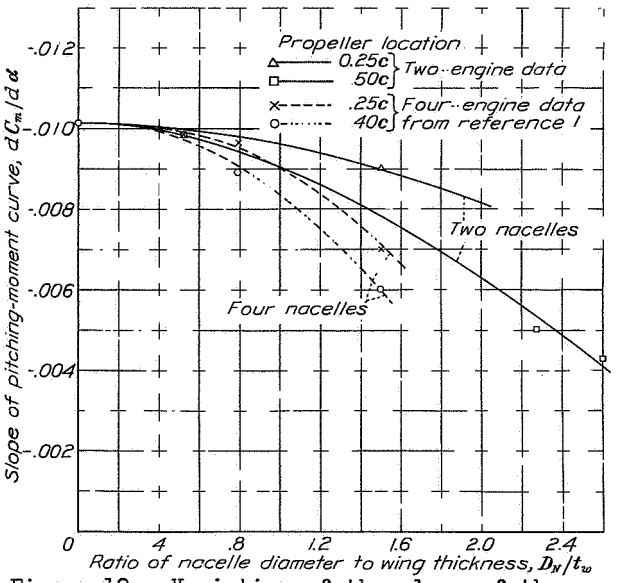

Figure 18.- Variation of the slope of the pitching-moment curve of the model for various nacelle sizes.

L-425

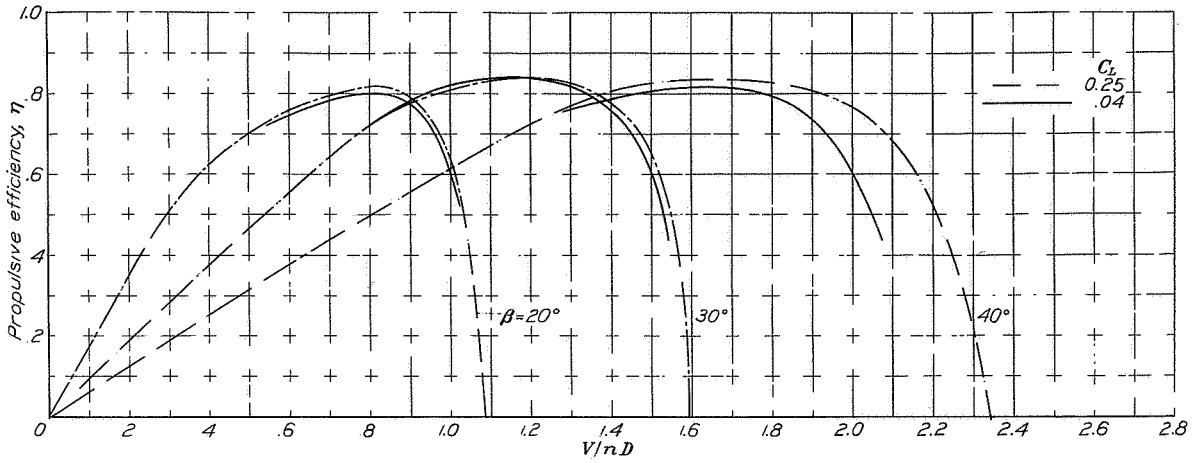

Figure 19.- Variation of propulsive efficiency with blade angle for the 20 inch nacelles in center line position. 0.25c propeller location; air flowing through cowling.

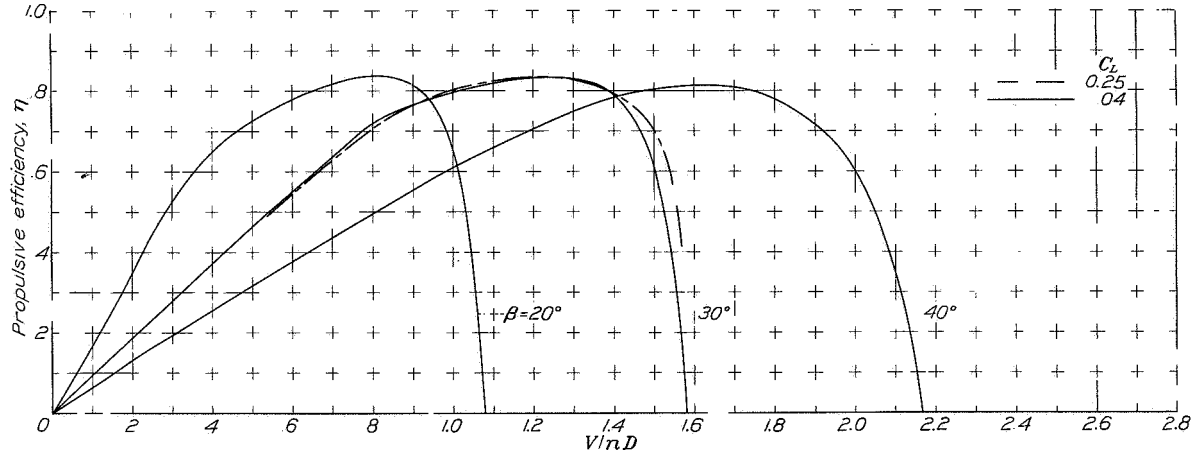

Figure 20 - Variation of propulsive efficiency with blade angle for the 20-inch nacelles in low position. 0.25c propeller location; air flowing through cowling.

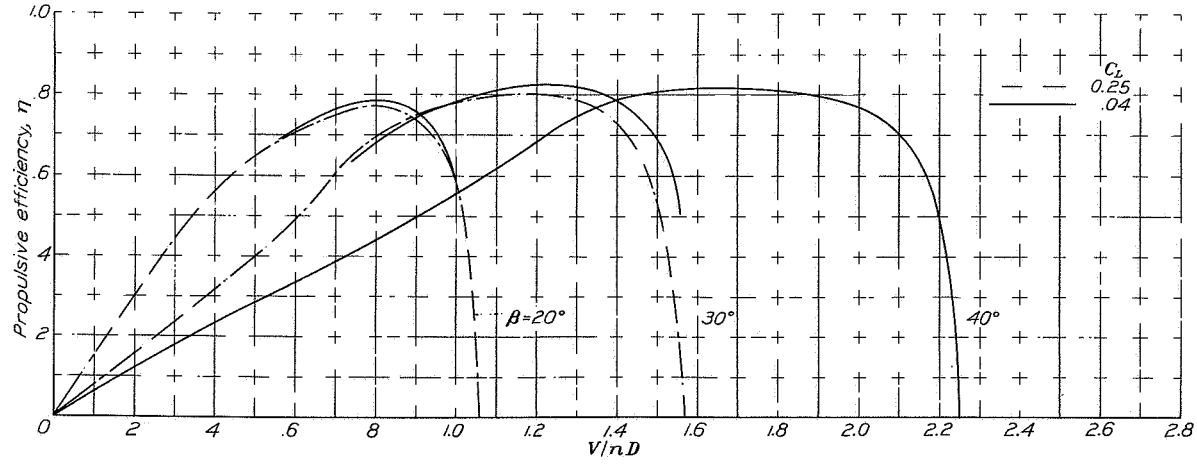

Figure 21.- Variation of propulsive efficiency with blade angle for the 30.4-inch nacelles 0.50c propeller location; air flowing through cowling.

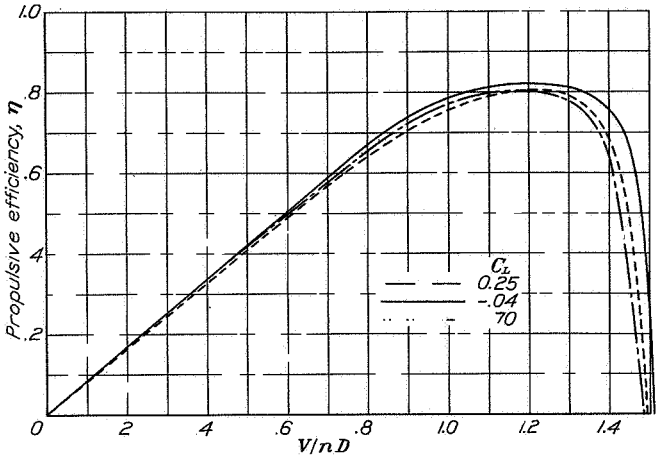

Figure 22.- Variation of propulsive efficiency with lift coefficient for the 34.7-inch nacelles. 0.50c propeller location; β, 300; air flowing through cowling.

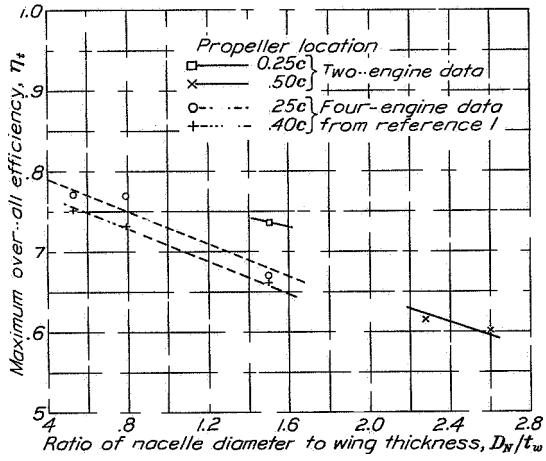

Figure 23.- Variation of maximum over-all efficiency with nacelle size. C_L, 0.25; β, approximately 30°; air flowing through cowling.

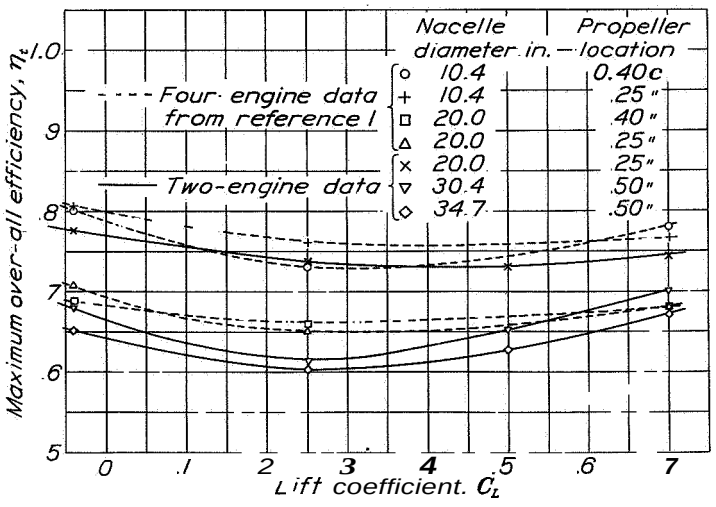

Figure 24.- Variation of maximum over-all efficiency with lift coefficient. Various nacelle arrangements; β, approximately 30°.

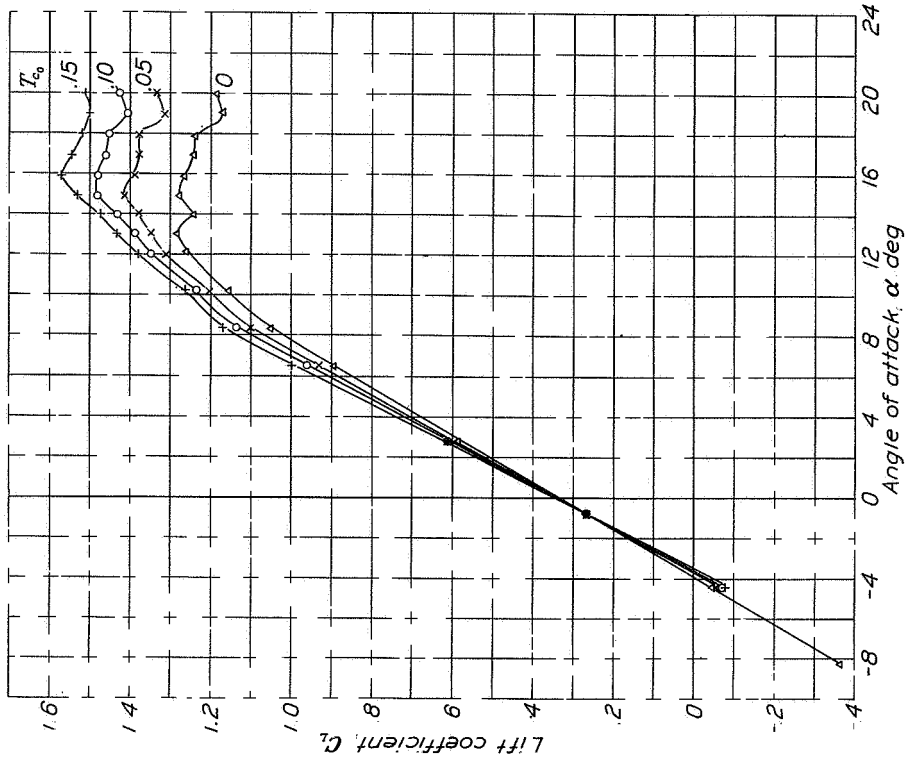

Figure 26.- Effect of propeller operation on lift coefficient of the model for various index thrust coefficients. The 34.7-inch nacelles; 0.50c propeller location; $\delta_f = 0°$.

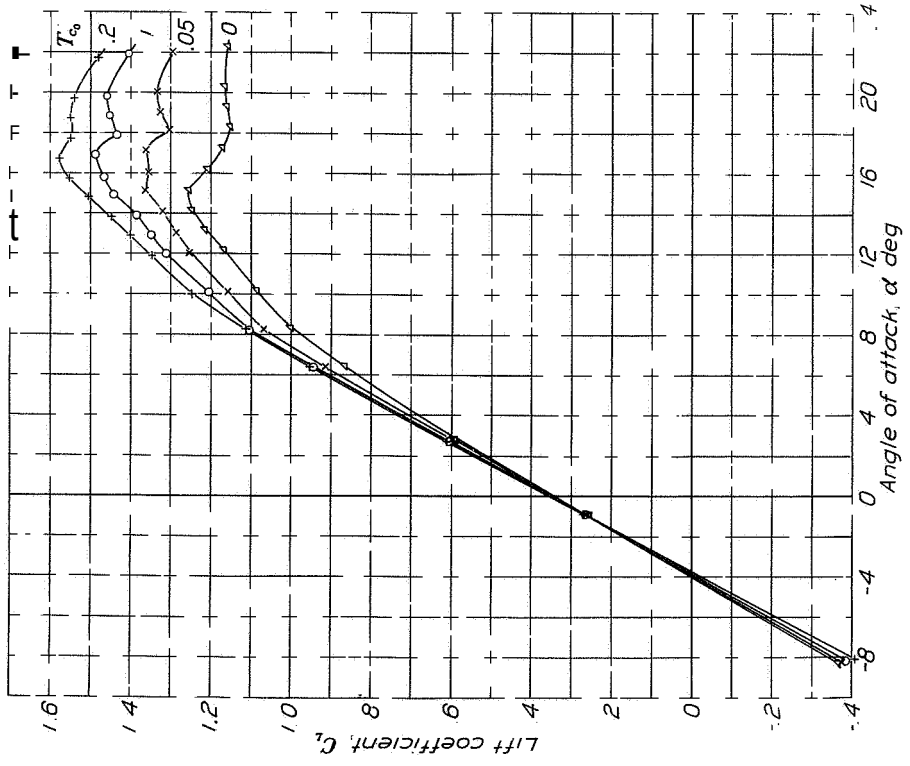

Figure 25.- Effect of propeller operation on lift coefficient of the model for various index thrust coefficients. The 20-inch nacelles in low position; 0.25c propeller location; $\delta_f = 0°$.

L-428

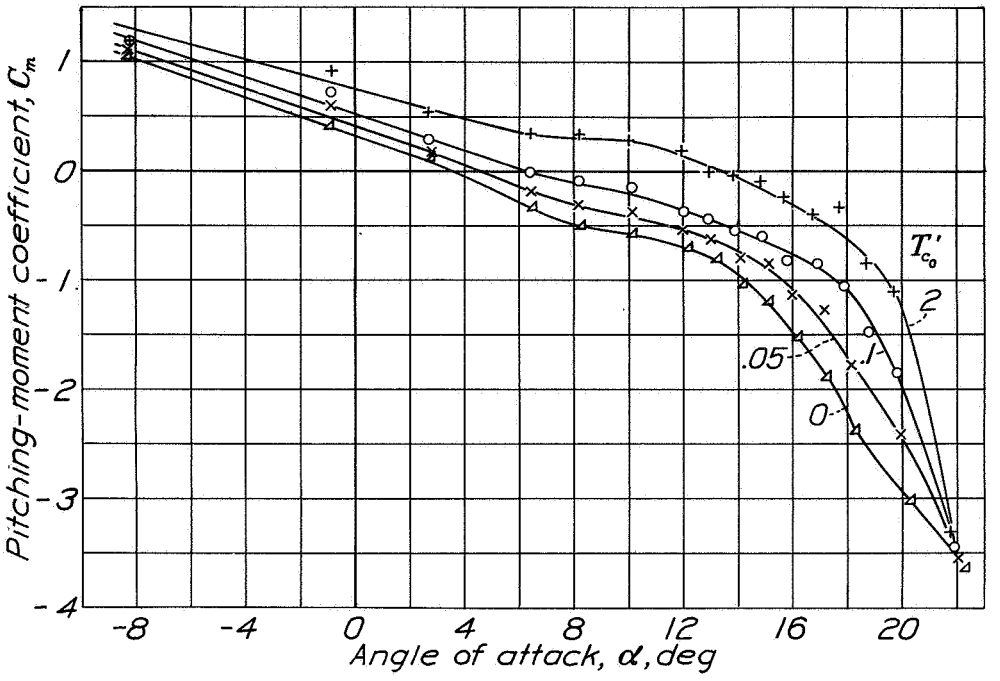

Figure 27.- Variation of pitching-moment coefficient of the model with index thrust coefficient. The 20-inch nacelles in center-line position. 0.25c propeller location.

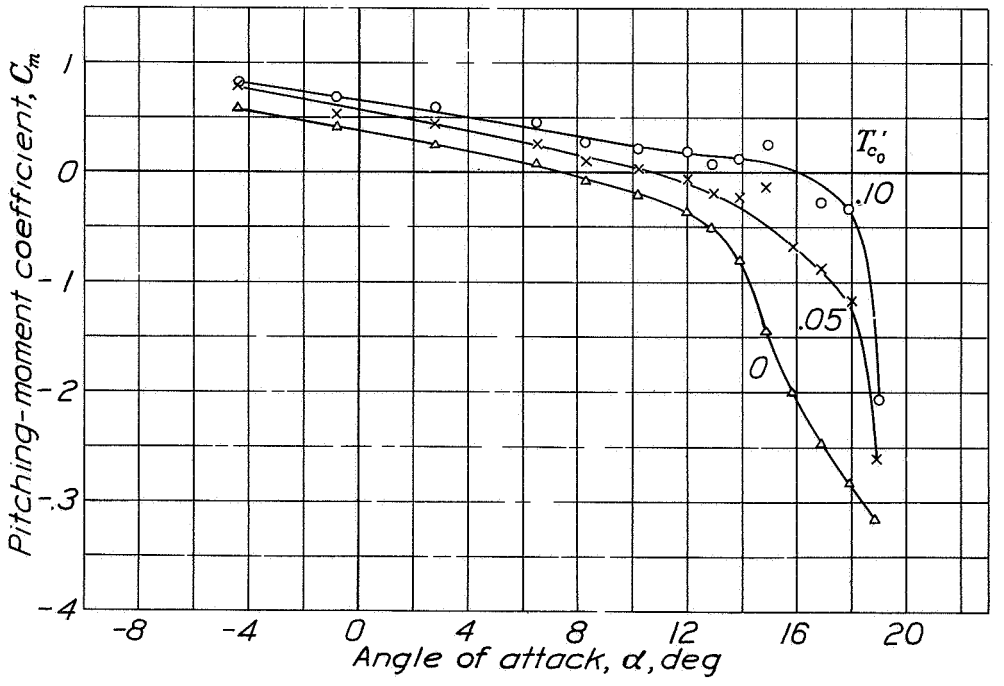

Figure 28.- Variation of pitching-moment coefficient of the model with index thrust coefficient, The 34.7-inch nacelles; 0.50c propeller location.

L-428

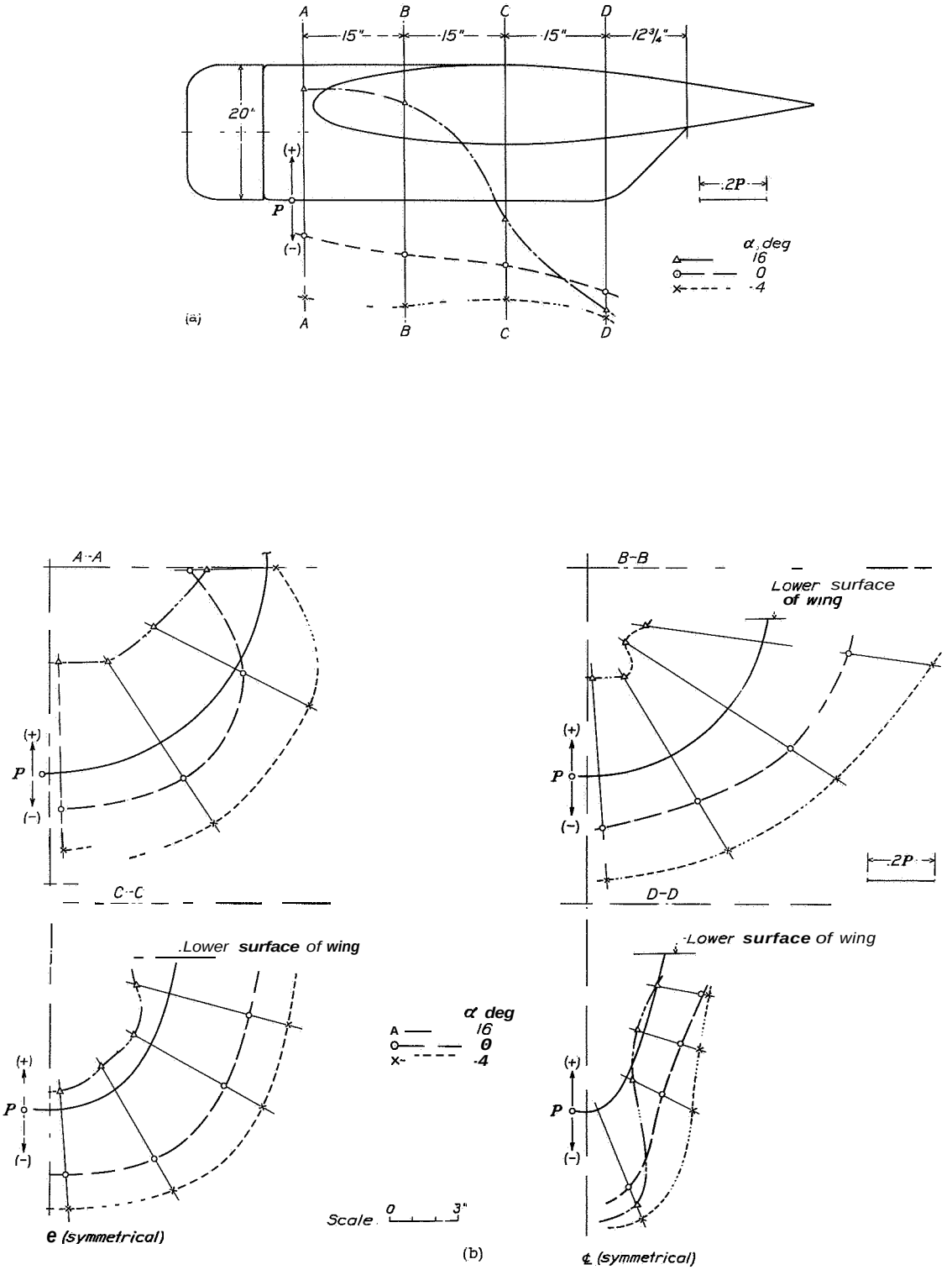

(a) Longitudinal sections. (b) Transverse sections.

Figure 29.- Pressure distribution for the 20-inch nacelles in low position.

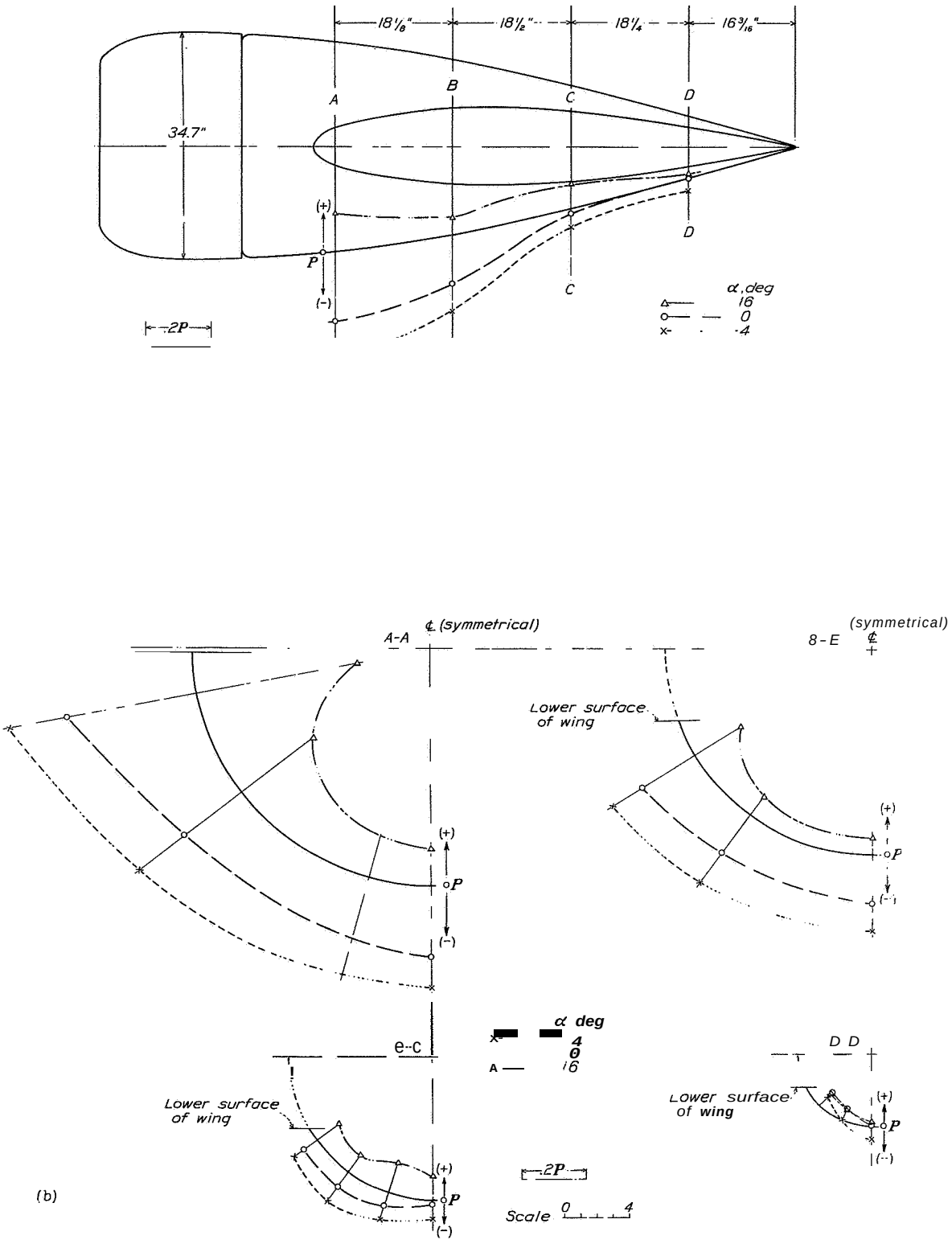

(a) Longitudinal sections. (b) Transverse sections.

Figure 30.- Pressure distribution for the 34.7-inch nacelles.